SciMedCentral

JSM Nanotechnology & Nanomedicine

Research Article

Bis-methanofullerene Trisphosphonic Acid as Matrix for Cytochrome c Immobilization

Melnikova NB*, Kochetkov EN, Gubskay VP, Fasleeva GM, Gilmutdinova AA, Islamova LN, Nizameev IR, Kadirov MK, and Nuretdinov IA

Department of pharmaceutical chemistry, Nizhny Novgorod State Medical Academy, Russia

***Corresponding author**

Melnikova NB, Department of pharmaceutical chemistry, Nizhny Novgorod State Medical Academy, Russia Federation, 603600, Nizhny Novgorod, Minin sq, 10/1. Russia, Tel: 79023092298; Email: melnikovanb@gmail.com

Submitted: 10 July 2017

Accepted: 24 July 2017

Published: 27 July 2017

ISSN: 2334-1815

Keywords

- Bis-methanofullerene tris-phosphonic acid; Cytochrome c; Langmuir monolayers; Nitric oxide

Abstract

The interaction between bis-methanofullerene tris-phosphonic acid (FTPA) and cytochrome c (cyt c) by using Langmuir-Shaeffer monolayers technique combined with AFM was studied. The FTPA molecules form stable Langmuir monolayers on the subphase of aqueous cyt c solution in contrast to the surface film of an island type under water. The values of limiting area A_0 of FTPA in monolayers depend on cyt c concentration in the subphase and are increased from 0,5 nm^2 ($C_{cyt\,c}$=1 mg·l^{-1}) up to 2,6 nm^2 ($C_{cyt\,c}$=10 mg·l^{-1}). The compressibility modulus $\tilde{N}_S^{-1}$ study reveals that the immobilization of cyt c in FTPA monolayers may change the surface film fluidization. AFM photos of transferring FTPA monolayers suggest the immobilization of cyt c into FTPA. It has been shown that cyt c into FTPA film can be able to act as an oxidant in the reaction with nitric oxide.

INTRODUCTION

Metalloprotein cytochrome *c* plays an important role *in vivo* by participating in the respiratory chain due to the course of redox processes in cyt c^{2+} /cyt c^{3+} metalloprotein [1], acting as a signal molecule of apoptosis after binding of reactive oxygen species. In fact, cyt *c* acts as a marker of biochemical reaction in the organism and it also may be a potential component of biosensors on the reaction species, including nitric oxide, nitrates and various reactive oxygen species [2-4]. The matrix for the immobilization of the metalloprotein is the main problem for development of redox-process tests, involving cyt *c* for the biomimetic study of the interaction of cyt *c* and reactive oxygen forms.

The fundamental requirements applicable to protein matrix include: strong chemical, biological and mechanical resistances, sufficient penetration for a metalloprotein and a substrate, a high specific surface area, sorption capacity, the possibility of obtaining in convenient technological form (monolayers, films and etc), optimal balance of hydrophilic/lipophilic properties. A number of materials as potential matrix are offered, among them gelatin, graphene, kaolin, fullerenes, calixarenes and others [5-10].

Fullerenes and their derivatives are non-conventional materials for preparing of matrix which is able to immobilize organic molecules, proteins, including cyt *c*, due to the reducing electrochemical properties and the ability to accept electrons [11-14]. In this study, 1-bis-methanofullerene tris-phosphonic acid (FTPA) was studied as a potential matrix for the immobilization of cyt *c.* The reactivity of cyt *c* in monolayers and films of FTPA was evaluated by reaction with nitric oxide.The ability of FTPA to immobilize was compared with its analogue – ethyl ester of FTPA ($(OEt)_5$-FTPA)

The choice of the phosphonic fullerene derivative for the immobilization of the metalloprotein is due to the fact that, the phosphonate group in SAM's is most favorable for electron transport in the cyt *c* [5], and contributes to a less conformational distortion of the cyt *c*. Besides, the phosphonate derivatives of fullerene are close to the phospholipids of the membrane in the cell, which increases the possibility of conducting biomimetic studies.

The high ability to aggregate of fullerene derivatives is the important problem of obtaining Langmuir films. The presence of phosphonate groups makes to control the structure of the monolayer by varying of the sub phase. In this connection, important attention is paid to the conditions for the formation of stable monolayers of phosphonate fullerenes on the water subphase and on a solid template.

EXPERIMENTAL

General

Solvents (analytical grade), cytochrome *c* from bovine heart (mol wt 12327 Da) were purchased from Sigma-Aldrich and used without further purification.

Synthesis of cis-1-bis-methanofullerene tris-phosphonic acid ethyl ester $(OEt)_5$-FTPA

([61,62-bis-(diethylphosphono)-phosphonic acid]bis-methanofullerene ethyl ester) and **of cis-1-bis-methanofullerene tris-phosphonic acid FTPA** ([61,62-bis-(tetra-hydroxy-bis-phosphono)-phosphonic acid] bis-methanofullerene) were described in supporting S1 and S2, respectively.

Subphase for forming monolayers

61,62-[bis-diethylphosphonic acid ethyl ester] bis-methano [60] fullerene $(OEt)_5$-FTPA was dissolved in chloroform. Firstly, fullerene trisphosphonic acid, FTPA was dissolved in DMSO then chloroform at DMSO: $CHCl_3$=3:7 ratio was added [2- 4]. 10^{-4} M solution of fullerenes was used.

Langmuir films

Langmuir film experiments were provided with KSV Nima 112D system using deionized water (resistivity >15 MΩ cm, Simplicity, Millipore Inc.) with 5,5 pH at 20 ± 1^0C as a subphase. For registration the surface pressure–area (π–A) isotherms the Wilhelmy plate method was used.

Spreading time and compression speed were chosen to provide as low hysteresis of the films as possible. Compression of the film was provided in continuous mode at a speed rate 60 $cm^2 \cdot min^{-1}$ by two symmetric frames. 20 μl of $(OEt)_5$-FTPA or FTPA solution were spreaded on the aqueous subphase with a chromatographic microsyringe in several stages; 30-40 min was allowed for evaporation of the solvent and equilibration of the amphiphiles on the interface. (0,6-1,2). 10^{-8} mol of $(OEt)_5$-FTPA and FTPA were spreaded on the substrate surface.

Substrate pretreatment and solution preparation

Quartz plates used as substrates for the LS deposition were preliminary cleaned by incubation in the $K_2Cr_2O_7$ - H_2SO_4 solution over 4 h at room temperature and abundantly rinsed with deionized water. The ITO plates were sonicated in chloroform and ethanol for 30 min and then also rinsed with deionized water. Then all substrates were dried at 150^0C during 3 hours.

Langmuir shaeffer (LS) transfer

LS depositions were carried out using a horizontal dip coating system at a surface tension π = 10 $mN \cdot m^{-1}$ onto quartz, indium tin oxide (ITO). The transferred films were washed by deionized water and then were dried in vacuum during 8 h.

UV-vis analysis

UV-vis spectra of transferred films on quartz substrate were recorded by UV-vis spectrometer "Shimadzu UV-1800" in the wavelength range 187-800 nm (standard – quartz).

Atomic force microscopy (AFM) imaging and AFM measurements

AFM visualization of transferred films was carried out by scanning probe microscopy MultiMode V (Veeco instruments Inc, USA) using silicon cantilevers RTESP (Veeco instruments Inc, USA) with nominal spring constants of 40 $N \cdot m^{-1}$ (tip curvature radius is of 10-13 nm). Images were captured with the following feedback settings: integral gain – 0,5÷1, the proportional gain - 5÷10. The scan rate was maintained in the range of 1-2 Hz. Distances in lateral dimensions were calibrated by imaging special calibration grid (STR3-1800P, VLSI Standards Inc.) in the temperature range 20-60°C. Distances normal to the surface were calibrated by measuring the depth of the bars of the same grid. The nonlinearity of the piezoelectric crystal has not been observed in this range. The antivibration system (SG0508) was used to eliminate external distortions. Imaging of transferred films was obtained using discontinuous contact AFM techniques and performed at low force set points.

RESULTS AND DISCUSSION

Figure 1 shows the spreading -A-isotherms of FTPA and $(OEt)_5$-FTPA at the air-aqueous solution interphase at 20^0C, respectively. The cyt *c* concentration was varied from 0 to 30 $mg \cdot l^{-1}$ into aqueous subphase. Table 1 lists the corresponding characteristic parameters.

The surface pressure of FTPA starts to increase at a molecular area about 0,3 nm^2. This behavior can be explained in terms of surface aggregation such as C_{60} islands formation, which arises from the high cohesive energy of fullerenes core and hence strong intermolecular attractive interactions. The FTPA islands then can be able to coagulate and to form flocs at the interface by Van der Waals interaction, considering that the solubility of FTPA in the aqueous buffer solution at pH 9 is 1% approximately.

This explanation was supported by the spreading isotherm of water-insoluble $(OEt)_5$-FTPA monolayers (Figure 1, curve 6). In this case, the limiting area per molecules is about 0,75 nm^2,which is estimated by extrapolating the approximate straight part of A-isotherm to zero pressure. This value of A_0 is close to theoretical value calculated for fullerene core which is equal 0,87 nm^2 [15]. Schematic illustration of FTPA molecules at the water-air interface are presented on Figure 2.

There is a significant cyt *c* effect on spreading isotherms both on the position and on the shape of the curves. When the amount of cyt *c* is equal or more than 0,5 $mg \cdot l^{-1}$, the overall isotherms show a larger molecular area than pure FTPA due to the adsorption of cyt *c* on FTPA monolayer (Figure 1a, Table 1).

In contrast to FTPA monolayers the limiting area of $(OEt)_5$-FTPA monolayers are changed insignificantly under cyt *c* influence (Figure 1b). It indicates that cyt *c* molecules could be better adsorbed on FTPA monolayer as compared with $(OEt)_5$-FTPA monolayer.

The interaction between cyt *c* and negatively charged FTPA monolayers was studied too by using compressibility analysis. We calculated compressibility modulus (elastic modulus) $\tilde{N}_S^{-1}$ from A curves (Figure 3).

The elastic modulus is an useful parameter for assessing elastic properties of Langmuir monolayers based on -A isotherms ($\tilde{N}_S^{-1} = -A \cdot \frac{d\pi}{dA}$). In general, a higher value of $\tilde{N}_S^{-1}$ indicates a less compressibility monolayer or membrane. The maximum value of the compressibility modulus $\tilde{N}_S^{-1}$ is referred to the highest packing molecules of the monolayer. Its value can be

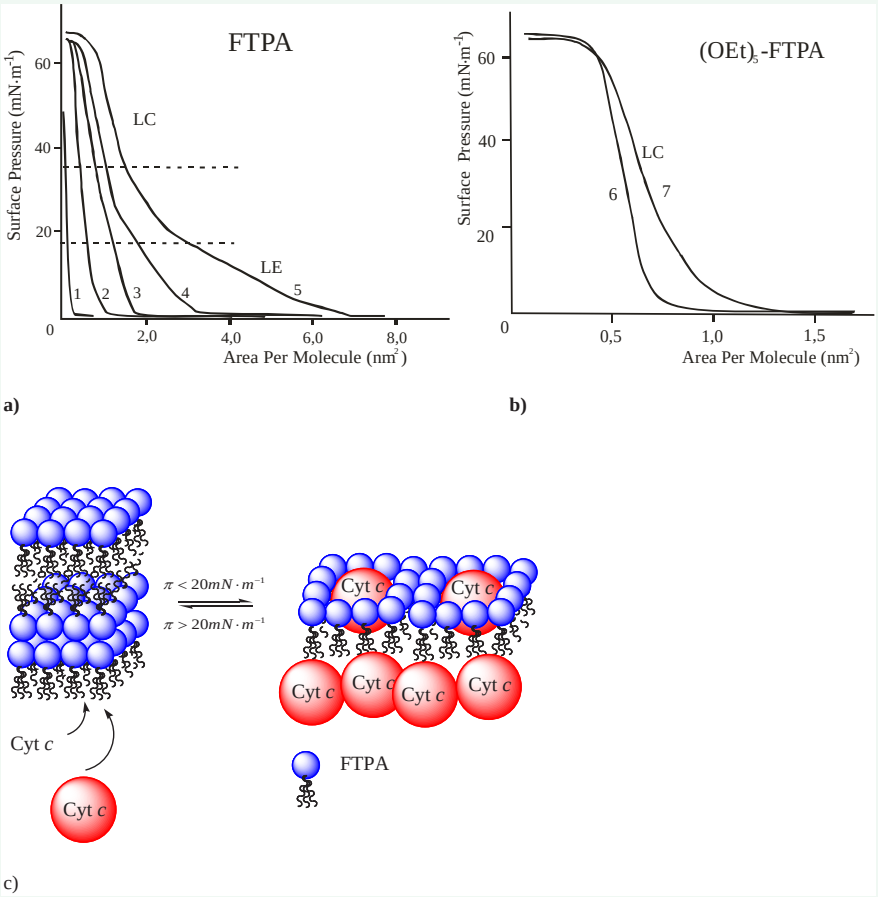

Figure 1 The π-A isotherms of FTPA (a) and $(OEt)_5$- FTPA (b) monolayers on aqueous cyt *c* containing subface; concentration cyt *c*: a) *1*- 0 mg·l^{-1}; *2*- 0,5 mg·l^{-1}; *3*- 1,0 mg·l^{-1} *cyt c*; *4*- 3,0 mg·l^{-1} *cyt c*; *5*- 10,0 mg·l^{-1}; b) 6 – 0 mg·l^{-1}; 7 - 30,0 mg·l^{-1}; c) Scheme of cyt *c* immobilization into FTPA monolayers.

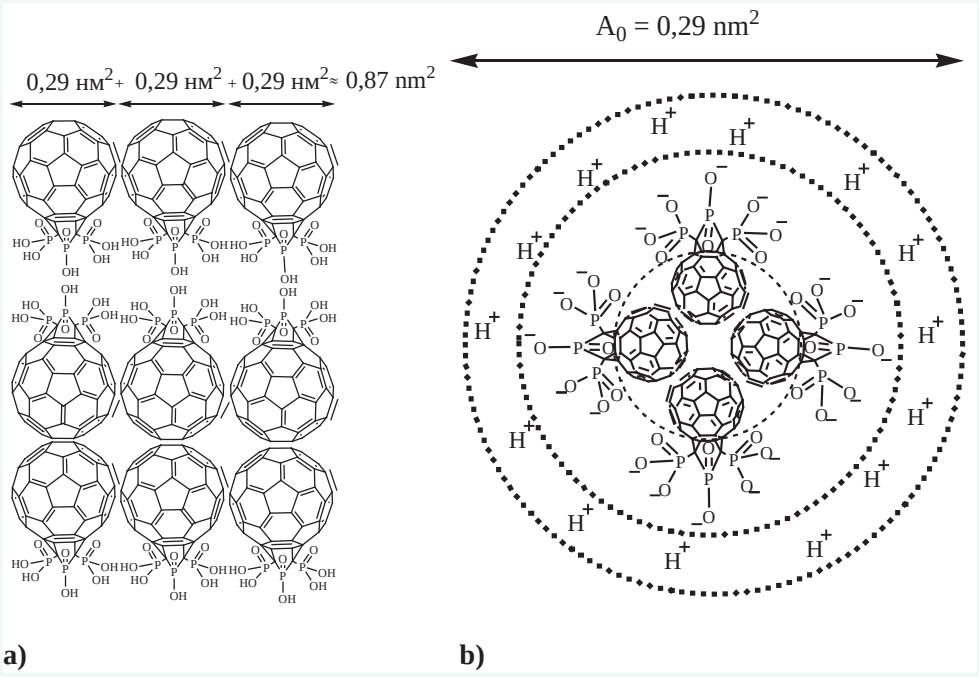

Figure 2 Schematic illustration of FTPA behavior at the air-water interface: a) the aggregation of FTPA molecules; b) the formation of floc.

Table 1: The properties of FTPA and $(OEt)_5$- FTPA monolayers.

Compound	Concentration cyt *c* (mg·l^{-1})	A_0 (nm^2)	$\tilde{N}_S^{-1}$ (mN·m^{-1})	ΔA (nm^2) *
FTPA	0,0	0,30±0,01	78±8	0,00
	0,1	0,43±0,01	82±12	0,14
	0,5	1,19±0,02	83±11	0,90
	1,0	1,36±0,04	82±14	1,07
	3,0	1,93±0,06	97±19	1,64
	5,0	2,34±0,08	94±23	2,06
	10,0	2,63±0,12	105±26	2,34
$(OEt)_5$-FTPA	0,0	0,69±0,02	145±7	0,00
	3,0	0,82±0,04	123±16	0,13
	5,0	0,90±0,02	135±9	0,21
	10,0	0,98±0,02	127±10	0,29
	30,0	0,94±0,03	122±9	0,25

*$\Delta A = A_{0\ cyt+ful} - A_{0\ ful}$ (nm^2), where ful - means FTPA or $(OEt)_5$- FTPA

used to characterize the phase state of the monolayer and to track the phase transitions during isothermal compression. $\tilde{N}_S^{-1}$ was changed approximately between 100 and 250 mN·m^{-1} for liquid-condensed monolayers and between 10 and 50 for liquid-expanded phases and is about for ideal surface film.

The $\tilde{N}_S^{-1}$ of pure FTPA and $(OEt)_5$-FTPA monolayers increase monotonously with increasing and attain a low maximum value 100 mN·m^{-1} for FTPA and 200 mN·m^{-1} for $(OEt)_5$-FTPA, respectively, which suggests a more rigid molecular structure of pure FTPA than of pure $(OEt)_5$-FTPA. The infection point can be ascribed either to a conformational change to the molecules in the monolayer or to a phase transition from liquid-condensed (LC on Figure 1) to a liquid-expanded phase (LE) as indicated by the decrease of $\tilde{N}_S^{-1}$ from 100 mN·m^{-1} to ~ 5 mN·m^{-1} in the case of FTPA and from 200 mN·m^{-1} to ~ 5 mN·m^{-1} for $(OEt)_5$-FTPA.

In this case of FTPA and $(OEt)_5$-FTPA monolayers on cyt *c*-containing subphase $\tilde{N}_S^{-1}$ was decreased approximately twice. The infection point is not due to such a phase transition as the difference in $\tilde{N}_S^{-1}$ (from 100 mN·m^{-1} to 80 mN·m^{-1} at the region π=15-50 mN·m^{-1}) indicates that the system $(OEt)_5$-FTPA-cyt *c* remains in liquid-condensed phase. More drastic changes of $\tilde{N}_S^{-1}$ was observed for FTPA-cyt *c* system, where liquid-condensed phase was formed at π=40-50 mN·m^{-1} with $\tilde{N}_S^{-1}$ ≈70-75 mN·m^{-1} only. At the surface pressure up to 45-50 mN·m^{-1} the mutual repulsion between water molecules and hydrophobic residues of cyt *c* molecules is stronger than their attraction (liquid-expanded films) then at more high π these large cyt *c* aggregations sink into the subphase from FTPA-cyt *c* monolayers during the sliding barrier sustained compression and liquid-condensed phase is formed.

The polar phosphonic acid moiety may be one deeper reason for this difference. Early it has been shown, that the interaction between cyt *c* and negatively charged phosphonic groups in phosphonic acid terminated self-assembled monolayers is mainly electrostatic interaction [12]. Therefore every phosphonic acid groups in FTPA monolayers should possess more than one unit negative charges in the neutral solution. This electrostatic interaction may promotes rearrangement of FTPA molecules in the monolayers on the aqueous cyt *c*-containing subphase from flocs to more loose structure (Figure1c). In this case molecular area per molecule in the FTPA-cyt *c*-monolayers may be changed from 0,29 nm^2 (floc) to 0,75 nm^2 (limiting area of $(OEt)_5$-FTPA less polar than FTPA).

At the first approximation if to assume that increase of limiting area of FTPA A due to cyt *c* only, the FTPA surface concentration which capable to adsorb cyt *c* may be quantified by N^s calculated as

$$N^S = \frac{1}{A_{o(water)}} - \frac{1}{A_{o(Cytc)}},$$

where

$$\frac{1}{A_{o(water)}} and \frac{1}{A_{o(Cytc)}}$$

are a surface concentration of FTPA on water and on cyt *c*-containing subphase, respectively.

The increase of FTPA limiting area A (Figure 4a) and surface concentration of FTPA, binding with cyt *c* on the film (Figure 4b) as a function of cyt *c* concentration in the aqueous subphase are shown on the Figure 4.

It has been shown that maximum surface concentration of FTPA, binding of cyt *c*, is equal to 5,0·10^{-10} mol·cm^{-2}, assuming that A_0=0,29 nm^2 for FTPA monolayers (Figure 4, curve 1). If FTPA molecules in the monolayers were reconstructed under influence of cyt *c* interaction with negatively charged phosphonic groups of FTPA, the limiting area may be taken as 0,75 nm^2 per molecule determinated for $(OEt)_5$-FTPA monolayers. In this case A_{max} may be as 1,52·10^{-10} mol·cm^{-2} (Figure 4, curve 1').

The surface concentration of cyt *c* onto FTPA monolayers has been studied by using UV-Vis spectra of FTPA monolayer transferred to quartz from aqueous subphase at 10 mN·m^{-1}. The pure FTPA monolayers were transferred from 0,05 M $CaCl_2$ solution that makes possible to get homogeneous thin film (AFM control).

Considering that the limiting area of pure of FTPA monolayer on 0,05 M $CaCl_2$ containing subphase is equal to 0,78 nm^2 similar the limiting area of $(OEt)_5$-FTPA, we suggest the re-arrangement the negatively charged FTPA molecules in the monolayer under influence positively charged Ca^{2+}. The same behavior may be proposed for FTPA on cyt *c* subphase, therefore the surface concentration of FTPA binding with cyt *c* can be expected as 1,52·10^{-10} mol·cm^2.

The spectra of transferred FTPA monolayers were similar as compared spectrum of FTPA in ethanol (Figure 5a). The blue shift of the band from 265 nm to 260 nm might be indicated that the FTPA molecules are tightly-packed on quartz surface. Linearly dependence of absorption at 260 nm (A_{260}) on number of transferred layers of FTPA (n) A_{260}=f(n) characterizes the good reproducibility of LS deposition.

When the FTPA monolayers were transferred to quartz from cyt *c* containing subphase, quartz plates were rinsed several times by water in order to remove any unbound cyt *c*. In UV-Vis spectra of resulting thin films, both the FTPA band at 260 nm

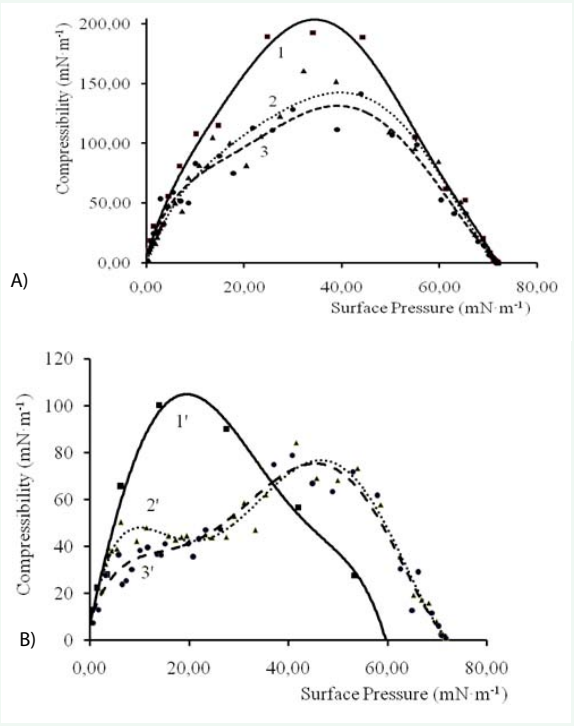

Figure 3 c_s^{-1} - π plot for $(OEt)_5$-FTPA - (**a**) and FTPA - monolayers (**b**) at the aqueous cyt *c*-containing subface; concentration of cyt *c*: **1,1'** - 0 mg·l^{-1}; **2,2'** - 5 mg·l^{-1}; **3,3'** - 10 mg·l^{-1}.

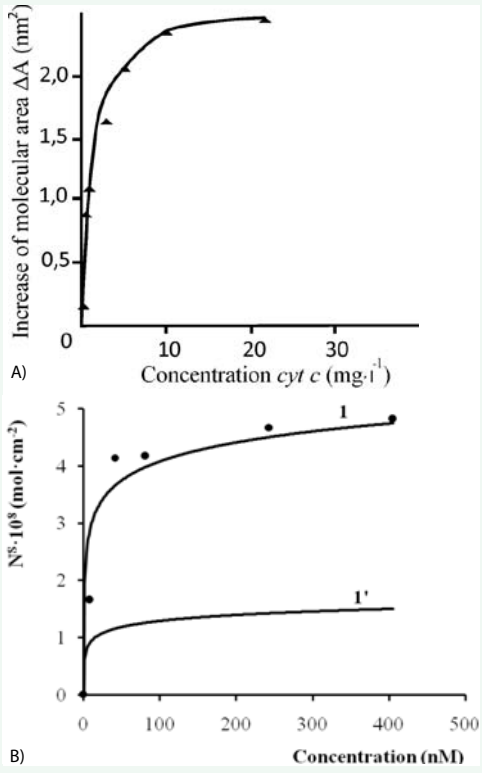

Figure 4 **The increase of FTPA limiting area ΔA (a) and the surface concentration of FTPA, binding with cyt c (b) as a function of cyt c concentration in the aqueous subphase.**

and the cyt *c* Soret and Q band located at 410 nm and 520 nm, respectively, were observed (Figure 5b). Insert shows linear dependence between absorption at 260 nm and 410 nm and number of transferred layers (n = 1-20).

For approximate analysis of cyt *c* content into FTPA film we have studied the dependence of absorption at 410 nm on cyt *c* concentration A = f ($C_{cyt\ c}$) in thin aqueous film. Thin films were obtained using 4 μL of aqueous solution containing cyt *c* in the range from 1,25 μg to 5,0 μg, which were closely placed between two quartz plates with common area equal 3,24 cm^2. This model system allows to estimate surface concentration of cyt *c* (MW = 12370 Da) in the range from $1{,}0\cdot10^{-11}$ mol·cm^{-2} to $12{,}5\cdot10^{-11}$ mol·cm^{-2}.

Figure 5c shows the absorption at 410 nm A_{410} versus surface concentration of cyt *c* in thin aqueous films between quartz plates. It has been estimated by using the calibration dependence A_{410} = f($C_{cyt\ c}$) in model system (Figure 5c) and the dependence A_{410} on number of transferred FTPA-cyt *c* layers that surface concentration of cyt *c* corresponds to $1{,}05\cdot10^{-11}$ mol·cm^{-2} for 1 layer and $2{,}12\cdot10^{-10}$ mol·cm^{-2} for 20 layers.

Cytochrome *c* from horse heart employed in the present study, is a low molecular weight heme protein with a single polypeptide chain of 104 amino acid residues covalently attached to the heme moiety. The shape of the cyt *c* molecule is roughly spherical with diameter of 3,4 nm which implies that the maximum surface coverage, i.e. that reached at hexagonal monolayers packing of adsorbed cyt *c* is $\Gamma_{max} \approx 1{,}7\cdot10^{-11}$ mol·cm^{-2}. One transferred monolayer consists of $1{,}05\cdot10^{-11}$ mol·cm^{-2} cyt *c* that determined by using "aqueous thin film" model and it is close to theoretical value ($1{,}7\cdot10^{-11}$ mol·cm^{-2}). The approximate appraising of molar ratio cyt *c:* FTPA in mixed monolayers gives 1:15 (if A_0 of FTPA=0,75 nm^2) and 1:50 (if A_0 of FTPA=0,29 nm^2).

A good agreement was found between the concentration of cyt *c* into thin film of FTPA-cyt *c* after 20 transfers which was determined as $2{,}12\cdot10^{-10}$ mol·cm^{-2} and the surface concentration of cyt *c* on fullerene film-modified electrode [12]. The surface concentration of cyt *c* was ranged from $0{,}5\cdot10^{-10}$ mol·cm^{-2} to $2{,}5\cdot10^{-10}$ mol·cm^{-2} it was measured by piezoelectric microgravimetry and $3{,}6 \pm 0{,}4\cdot10^{-10}$ mol·cm^{-2} determined by cyclic voltamperometry techniques.

The resulting FTPA-cyt *c* film consist of 20 transferred layers are very stable in water. The desorption of cyt *c* was observed under ascorbic acid action in aqueous solution. The desorption of cyt *c* depends on concentration of ascorbic acid (Figure 6). It may be explained that the immobilization of cyt *c* on negatively charged FTPA surface can be related to an increase in the negatively charge on FTPA surface in the presence of ascorbic acid.

The AFM images and height profiles of the 4 initial transferred FTPA monolayers onto the hydrophobic ITO substrate from water surface have shown that island type of the film was formed (Figure 7a,b). The island type of the FTPA film on the hydrophobic substrate due to the aggregation of monolayers on water surface and therefore the formation same structure of monolayers on solid. The roughness of 4 deposited films of FTPA is about 12 nm.

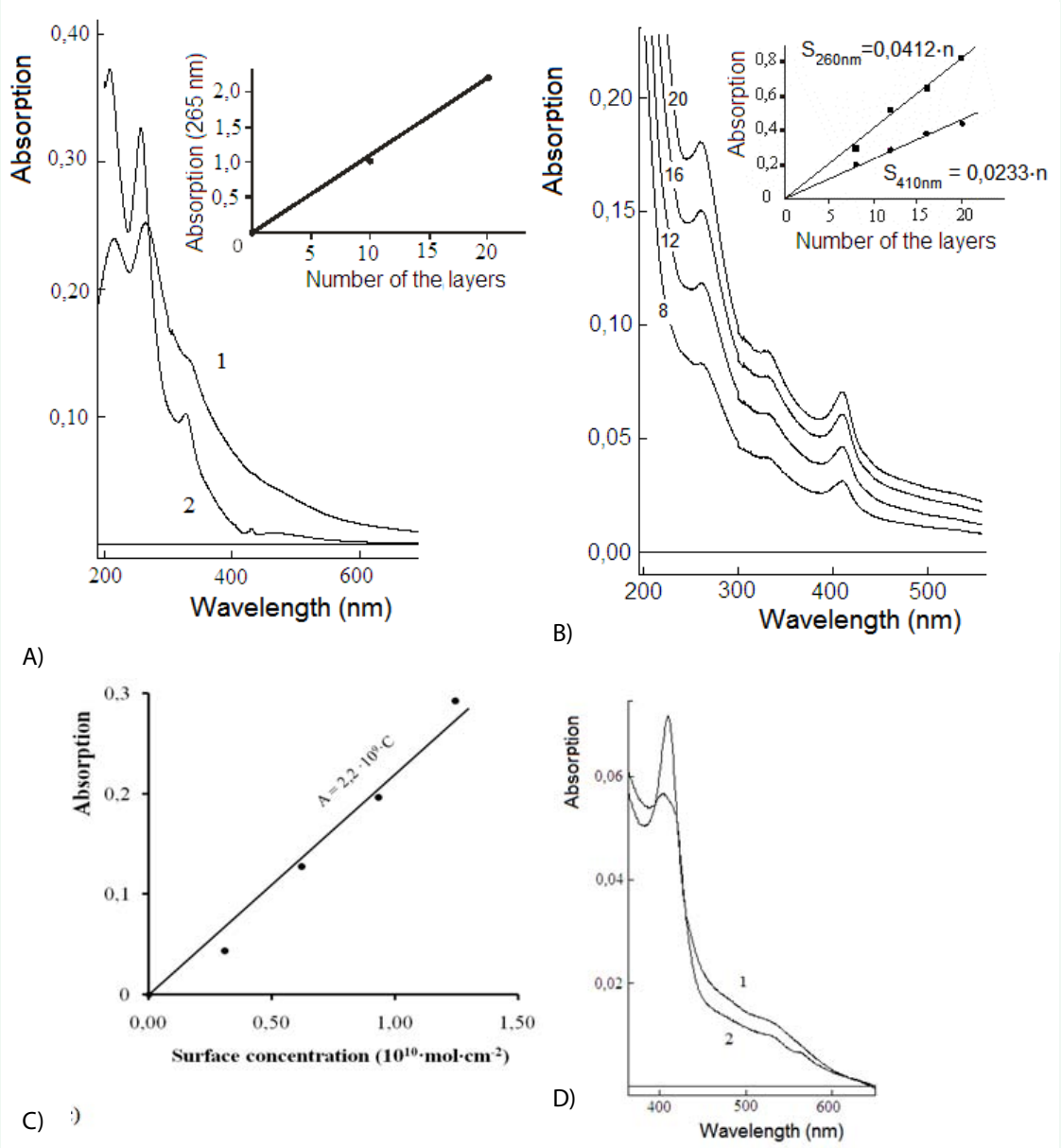

Figure 5 UV-vis spectra of FTPA: (a) monolayers transferred from 0,05 M CaCl2 containing a subphase onto quartz (1) by comparision with the ethanol solution of FTPA (2). The insert shows the dependence between the absorption at A260 and number of the transferred layers (n); (b) monolayers transferred from cyt c containing subphase on quartz (the number of the curves corresponds to the number of transferred monolayers); insert shows the dependence between absorption and the number of the layers; (c) absorption A410 versus the surface concentration of cyt c in the thin aqueous film between the plates and FTPA on quartz. (d) 40 monolayers of FTPA on quartz before (1) and after reaction (2) with gaseous NO.

The maximum of particle height distribution of the film surface significantly changes if 4 FTPA monolayers contain cyt *c* molecules. In this case the roughness increases from 12 nm to 40 nm in the presence of cyt *c* (Figure 7c) and the transfer of the 4 monolayers leads to the formation of a continuous film. The AFM data and high surface concentration of cyt *c* onto 20 layers ($2{,}12 \cdot 10^{-10}$ mol·cm^{-2}) make possible to use thin films of FTPA as a matrix for cyt *c* immobilization.

To estimate the effect of cyt *c* immobilization on its redox-property the obtained films were studied for the sensing of nitric oxide by UV-vis spectroscopy. The 40 transferred monolayers of FTPA-cyt *c* on quartz were contacted with gaseous nitric oxide. Short contact of the films with NO leads to the shift of the Soret band at 410 nm to 404 nm and the same time the absorption of this band is decreased, but α- and β- bands (Q-band) at 561 nm and 529 nm, respectively, are appeared (Figure 5d). This spectral picture is typical for nitrosyl complex of cyt c^{2+} (ferrichrome-NO) [16] (Figure 8).

CONCLUSION

In summary, we have demonstrated the immobilization of redox-active protein, cyt *c,* into bis-methanofullerene tris-phosphonic acid FTPA monolayers on cyt *c* containing aqueous

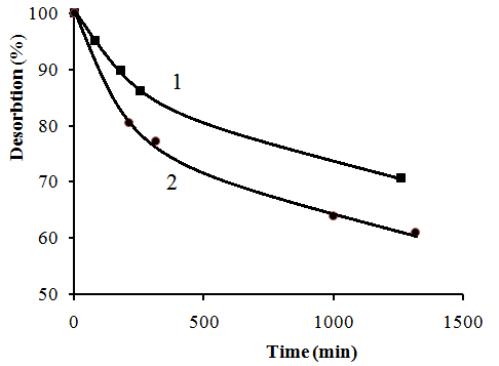

Figure 6 Desorption on cyt c from mixed film FTPA-cyt c under the action of 1·10-3 M (1) and 1·10-2 M (2) ascorbic acid in a time.

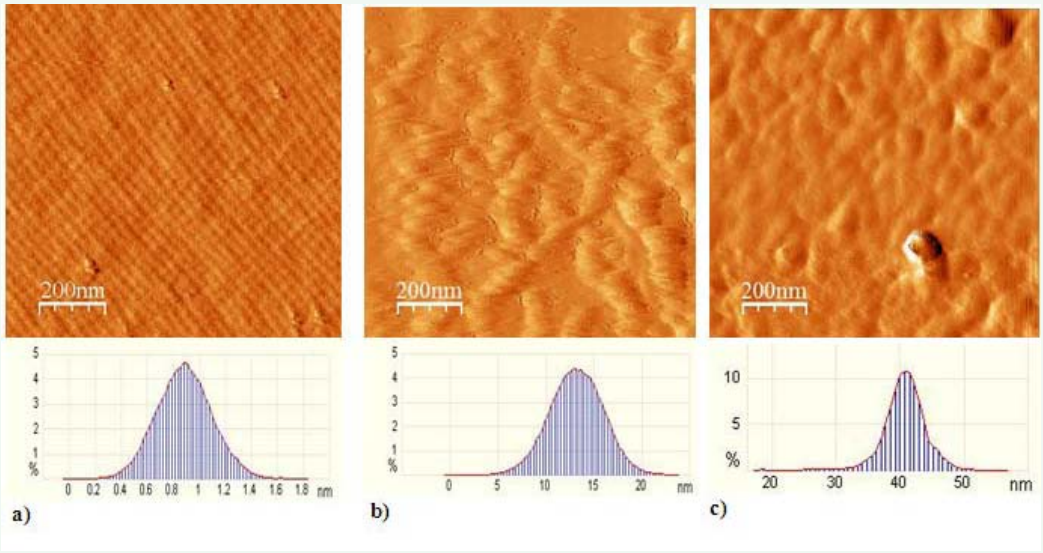

Figure 7 AFM visualization and surface properties of ITO substrate: **a)** without a film (clean substrate); **b)** with 4 LS monolayers transferred from H_2O; **c)** with 4 LS monolayers transferred from cyt *c* containing solution (10 mg·l^{-1}).

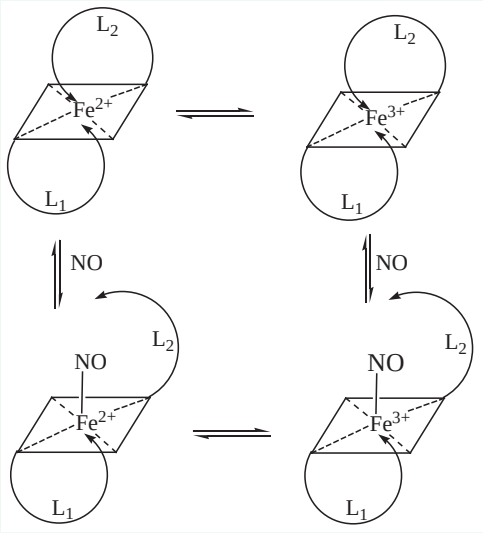

Figure 8 Scheme of cyt *c* nitrosilation by NO_{gas}.

subphase, while FTPA forms the island type film on pure water. The compressibility modulus $\tilde{N}_S^{-1}$ study reveals that the immobilization of cyt *c* into FTPA monolayers may change the surface film fluidization.

The surface cyt *c* concentration equaled $1{,}05 \cdot 10^{-11}$ mol·cm^{-2} (one monolayer) and 2,12·10-10 mol·cm^{-2} (20 monolayer) have been determined by using UV-vis spectra of thin layers of cyt *c* into quartz cuvette and transferred FTPA-cyt *c* layers onto quartz. It has been estimated by using UV-visible spectra that cytochrome *c* into FTPA film, which was transferred from cyt *c* containing aqueous subphase, can be able to act as an oxidant in the reaction with nitric oxide.

REFERENCES

1. Anastasia SD, Lidia G, Joanna D, Jerzy LG, Benjamin vder M, Willem HK. The kinetics of the reaction of nitrogen dioxide with iron (II)- and iron(III) cytochrome *c*. Free Rad Biol Med. 2014; 69: 172-180.
2. 2. Zhou Y, Zhi J, Zou Y, Zhang W, Lee ST. Direct Electrochemistry and Electrocatalytic Activity of Cytochrome *c* Covalently Immobilized on a Boron-Doped Nanocrystalline Diamond Electrode. Anal Chem. 2008; 80: 4141-4146.
3. Alvin Koh WC, Rahman MA, Choe ES, Lee DK, Shim YB. A Cytochrome ***c*** modified-conducting polymer microelectrode for monitoring in vivo changes in nitric oxide. Biosens Bioelectron. 2008; 23: 1374-1381.
4. Beissenhirtz MK, Scheller FW, Lisdat FA. Superoxide Sensor Based on a Multilayer Cytochrome *c* Electrode. Anal Chem. 2004; 76: 4665-4671.
5. Chen Y, Yang XJ, Guo LR, BoJi, Xia XH, Zheng LM. Direct electrochemistry of cytochrome *c* on a phosphonic acid terminated self-assembled monolayers. Talanta. 2009; 78: 248-252.
6. Zhang N, Xiangyu L, Ma W, Hu Y, Li F, Han D, Niu L. Direct electron transfer of cytochrome *c* at mono-dispersed and negatively charged perylene–graphene matrix. Talanta. 2013; 107: 195-202.
7. Wael KD, Belder SD, Vlierberghe SV, Steenberge GV, Dubruel P, Adriaens A. Electrochemical study of gelatin as a matrix for the immobilization of horse heart cytochrome *c*. Talanta. 2010; 82: 1980-1985.
8. Perhirin A, Kraffe E, Marty Y, Quentel F, Elies P, Gloaguen F. Electrochemistry of cytochrome *c* immobilized on cardiolipin-modified electrodes: A probe for protein–lipid interactions. Biochimica et Biophysica Acta. 2013; 1830: 2798-2803.
9. Sato Y, FMizutani F. Electrochemical responses of cytochrome *c* on a gold electrode modified with mixed monolayers of 3-mercaptopropionic acid and n-alkanethiol. J Electroanalyt Chem. 1997; 438: 99-104.
10. Castellini E, Bernini F, Berto M, Borsari M, Sola M, Ranieri A. Solvent tunes the peroxidase activity of cytochrome *c* immobilized on kaolinite. Applied Clay Science. 2015; 118: 316-324.
11. Yu B, Shu X, Cong H, Chen X, Liu H, Yuan H, et al. Self-assembled covalent capillary coating of diazoresin/carboxyl fullerene for analysis of proteins by capillary electrophoresis and a comparison with diazoresin/graphene oxide coating. J Chromatograp. 2016; 1437: 226-233.
12. D'Souza F, Rogers LM, O'Dell ES, Kochman A, Kutner W. Immobilization and electrochemical redox behavior of cytochrome *c* on fullerene film-modified electrodes. Bioelectrochem. 2005; 66: 35-40.
13. Nobuyuki H, Takayo I, Masazo N. Immobilization and cleavage of DNA at cationic, self-assembled monolayers containing C_{60} on gold. Chem Commun. 1997; 1507-1508.
14. Pramod N, Marcello C, Vasilis GG, Mark SM, John EA, Leonidas GB. Hybrid Nanoparticles Based on Organized Protein Immobilization on Fullerenes. Bioconjugate Chem. 2004; 15: 12-15.
15. Yeletskiy AV, Smirnov BM. Fullereny i struktury ugleroda, Uspekhi Fizicheskikh nauk. 1995; 165: 977-1009.
16. Christopher MS, Benjamin G, Joan BM. Nitrosylation of Cytochrome *c* during Apoptosis. J Biol Chem. 2003; 278: 18265-18270.

Cite this article

Melnikova NB, Kochetkov EN, Gubskay VP, Fasleeva GM, Gilmutdinova AA, et al. (2017) Bis-methanofullerene Trisphosphonic Acid as Matrix for Cytochrome c Immobilization. JSM Nanotechnol Nanomed 5(2): 1051.